Algal Research 33 (2018) 266–276

Contents lists available at ScienceDirect

Algal Research

journal homepage: www.elsevier.com/locate/algal

Zinc removal by *Chlorella* sp. biomass and harvesting with low cost magnetic particles

Gisela Ferraro[a], Regina M. Toranzo[a], Delfina M. Castiglioni[a], Enio Lima Jr[b], Marcelo Vasquez Mansilla[b], Nicolas A. Fellenz[c], Roberto D. Zysler[b], Daniel M. Pasquevich[a], Carolina Bagnato[a,*]

[a] Instituto de Energía y Desarrollo Sustentable, Centro Atómico Bariloche, Av. Bustillo 9500, CP8400 Bariloche, Argentina
[b] Laboratorio Resonancias Magnéticas, Centro Atómico Bariloche, Av. Bustillo 9500, CP8400 Bariloche, Argentina
[c] Centro de Investigación y Transferencia de Río Negro, Av. Don Bosco 500, CP8500 Viedma, Argentina

ARTICLE INFO

Keywords:
Algal biomass harvesting
Metal remediation
Magnetic particles
Natural magnetic clay
Stationary phase
Exponential phase

ABSTRACT

Remediation of an environment affected by metals based on the use of algae is an important technological breakthrough, where biomass harvesting is the limiting key-point. In this research, iron oxide particles (IOPs) and natural magnetic clay (NMC) coated with polyethilenimine (PEI) were successfully applied in the harvesting of *Chlorella* sp. coupled to the remediation of zinc ions with harvesting efficiencies > 94%. Even though the presence of the metal did not affect the harvesting process, adding IOPs induced a metal displacement which increased zinc concentration upon harvesting. Contrary to that, Clay-PEI functionalized (NMCP) particles increased the amount of removed metal after harvesting. From these results it can be concluded that both tested particles are suitable for harvesting algal biomass and only NMCP are compatible with metal remediation.

1. Introduction

During the last decades algal biomass has been found to have multiple biotechnological applications, such as wastewater bioremediation and biofuel production [1–5]. In this context, several algae species have been characterized in their capacity for massive cultivation, lipid yield and metal removal from different water matrices [6,7]. Due to the diluted nature of algae cultures and the required downstream processing biomass concentration is necessary. Even though technologies have evolved, biomass harvesting is still a bottleneck that might jeopardize the complete development and application of algae biotechnologies [8–12]. In recent years, the idea of using magnetic particles for algae biomass harvesting has drawn attention and a series of articles have been published describing the properties of such magnetic particles and their efficient application for harvesting [13–16]. Some results describe particle-cell surface interaction and how the harvesting performance is affected by particle functionalization, pH and ionic strength changes [14,15,17,18]. This method has been successfully applied in the harvesting of different algae species [19–22]. In addition, magnetic harvesting offers the advantage of simplicity, low energy consumption, short time execution and the possibility to re-use magnetic particles and culture medium [16,20,23,24]. One of the unanswered issues about the magnetic harvesting is its efficiency on biomass recovery during metal bioremediation.

Human activities and industrial processes have led to worldwide heavy metal pollution. Water and soil contamination by zinc is mainly due to the release of wastewater from the galvanization and electroplating industries [25–27]. Although zinc is an essential cofactor for some enzymatic activities, in high doses it becomes toxic (100–500 mg/day) [25]. This leads to a major need for remediation of contaminated soils and water as well as industrial wastewater treatment. Algal biomass has proven to be very effective for metal removal from water [3,28–30]. The biosorption capacity for heavy metal ions has been essentially attributed to the presence of various functional groups on the algal cell surface such as hydroxyl, phosphoryl, amino, carboxyl and sulphydryl, which confer negative charge to the cell surface [3,31]. However, metal adsorption could modify functional groups availability and thus cells surface charge affecting magnetic harvesting. In this regard testing metal removal and magnetic harvesting compatibility is needed.

This work focuses on finding an appropriate system for metal removal coupled to an efficient harvesting method. Therefore, the

Abbreviations: DLS, Dynamic Light Scattering; FT-IR, Fourier Transform Infrared spectroscopy; IOPs, Iron Oxide Particles; NMC, Natural Magnetic Clay; PEI, Polyethylenimine; NMCP, Natural Magnetic Clay-PEI; SEM, Scanning Electron Microscopy; XRD, X-Ray Diffraction

* Corresponding author.
E-mail address: carolina.bagnato@cab.cnea.gov.ar (C. Bagnato).

https://doi.org/10.1016/j.algal.2018.05.022
Received 9 April 2018; Received in revised form 24 May 2018; Accepted 27 May 2018

compatibility of metal removal and magnetic harvesting is tested. *Chlorella* cells are employed to study zinc removal and magnetic harvesting using two different magnetic materials: 1) Iron Oxide Particles (IOPs) obtained by co-precipitation method and 2) Natural Magnetic Clay (NMC). Magnetic material characterization, harvesting assays, zinc removal at different metal concentration and the compatibility of both processes are analyzed. ζ-potential changes and the interplay of cell surface functional groups due to the presence of zinc are studied as well. Another issue analyzed in this work is if the physiological state of the algae cultures affects the metal remediation and the magnetic harvesting.

2. Materials and methods

2.1. Magnetic particles synthesis and preparation

2.1.1. Magnetic iron oxide particles synthesis by the co-precipitation method

The magnetic iron oxide particles were synthesized by precipitating the particles from an aqueous mixture of iron salts composed by $FeCl_3.6H_2O$ and $FeSO_4.7H_2O$, with a molar ratio $Fe^{3+}/Fe^{2+} = 2$. Precipitation was induced by addition of NH_4OH (25%) at room temperature under magnetic stirring. The brownish product powder was separated by filtration and exhaustively washed with water and ethanol. The final obtained solid was denoted as IOPs for Iron Oxide Particles.

2.1.2. Preparation and functionalization of natural magnetic clay particles

The magnetic particles were prepared by high-energy ball-milling using as a starting material the natural magnetic powder obtained from the clay of Iloca beach in Chile (34°55′00″S 72°11′00″O) by magnetic separation. Milling was performed in a 8000D dual mixer/mill during 600 min and with a mass relation between Balls and Powder of 12:1. The as-milled powder was collected from the vial with acetone. The surface charge of the particles was changed after the milling using a rotary evaporator and dispersing 1 g of as-milled powder and 5 g of branched polyethylenimine (PEI, MW = 25.000, Sigma-Aldrich, USA) in 100 mL of citrate buffer (pH = 5.5) with the addition of 0.1 mL of TWEEN80. The solution was incubated in a rotary shaker during 24 h at 200 rpm and at 40 °C. After that, the magnetic particles coated with PEI were collected by magnetic separation.

2.2. Magnetic particles characterization

2.2.1. X-Ray diffraction (XRD)

The XRD patterns of the particles sample were measured using a Empyrean X-rayPW170 diffractometer (Phillips, The Netherlands) with CuKα radiation, between 2θ = 20–70° at steps of 0.02° with counting time of 2 s/step. Samples were conditioned by dispersing the powder on a sandblasted glass.

2.2.2. Hydrodynamic size and ζ-potential measurements

Hydrodynamic size and ζ-potential measurements were performed in the Dynamic Light Scattering (DLS) equipment ZetaSizer ZS90 (Malvern, United Kingdom). For hydrodynamic diameter, the measurements were performed with a scatter angle of 90° and using a standard polymeric cuvette. The particles were dispersed in deionized water. Three sets with an automatically calculated number of measurements were performed of each sample and the final results were obtained from the statistical analysis of these three sets. The ζ-potential measurements were performed for the particles dispersed in deionized water at pH 7 and for the cells in culture medium at pH 5.5 and pH 6.8 using standard polymeric cuvettes and an applied potential of 150 V.

2.2.3. Magnetic properties analysis

Magnetization curves as function of applied field up to 10 kOe were performed at room temperature in a commercial vibrating sample magnetometer (Lakeshore) calibrated with a Ni sphere. For the measurements, samples were conditioned by dispersing in a polymeric matrix to avoid the mechanical rotation.

2.3. Alga strain used and culture conditions

The strain *Chlorella* sp. 20A, was isolated from an avian farm wastewater treatment and kindly donated by Dr. Javier Fernandez Velasco, National University of Lujan. Algal cells were grown on modified Bold Medium without ethylenediaminetetracetic acid (EDTA), with reduced Zn^{2+} concentration (0.023 g/L ZnSO4. 7H2O) and at a pH of 5.5. Algal cells were cultured in 250 mL Erlenmeyer flasks with 100 mL medium on a rotary shaker at 21 °C under light vs. dark cycle of 14 h vs. 10 h respectively and at an irradiance of 80 μmol/m^2 s using cool light fluorescent and grolux lamps. Growth was monitored by cell count using a Neubauer chamber. All experiments regarding culturing, harvesting and metal removal were performed under sterile conditions.

2.4. Magnetic separation of algal biomass: experimental procedure

Magnetic separation was performed in 50 mL Erlenmeyer flasks with 10 mL modified Bold Medium inoculated with algae in both growth phases, exponential and stationary, to reach a density of 9×10^6 cells/mL. The magnetic particles were suspended in 5 mL of deionized water and dispersed by bath sonication for 5 min. The amount of magnetic particles necessary to obtain 90% harvesting efficiency was assessed in preliminary experiments. Algal cells and magnetic particles were mixed at 250 rpm for 5 min and exposed to a permanent NdFeB magnet (a disc with a diameter of 16 mm and 5 mm in thickness with a magnetic field of 8 kOe at the surface of the magnet) for 2 and 5 min. After exposure, a sample of supernatant was taken by means of a pipette while the Erlenmeyer was still placed next to the magnet. Algal cells remaining in the supernatant were counted under a light microscope using a Neubauer chamber and harvesting efficiency (E%) was calculated as follows: $E = [(A_0 - A_1)/A_0] \times 100$, where A_0 is the initial cell number of the algal suspension before separation and A_1 is the cell number of the supernatant after the magnetic separation. Due to the small cell size of *Chlorella* and short harvesting time, sedimentation of algae cells to the bottom of the Erlenmeyer was neglected. All experiments were performed in triplicate and presented results are mean values ± standard deviation.

2.5. Metal removal experiments

Metal removal experiments were performed in batch-like assays with algae cultures in both, exponential and stationary, growth phase. Zinc chloride ($ZnCl_2$) was dissolved in deionized water, to a final concentration of 2 g $ZnCl_2$/L (note that all zinc concentrations hereafter are expressed as mass of Zn^{2+}, and not as mass of $ZnCl_2$). Experiments were performed in 50 mL Erlenmeyer flasks with 10 mL of algal cells diluted in Bold Modified Medium to reach 9×10^6 cells/mL and Zn^{2+} initial concentration between 25 and 125 mg/L. After 24hs, a 1.5 mL sample was centrifuged for 10 min at 10000*g* and the supernatant was collected to determine Zn^{2+} ions concentration by using Inductively Coupled Plasma with optical emission spectrophotometer (ICP OES) Agilent 5110. The total Zn^{2+} removed by algal cells was calculated as the difference between the initial and the remaining Zn^{2+} concentration in the supernatant and expressed as metal removal efficiency. After taking the sample for the determination of Zn^{2+} concentration, algal cells were harvested as described in the previous section. Metal uptake experiments were carried out in triplicate, and the results are expressed as mean values ± standard deviation. All materials used to handle and grow the algae were previously rinsed with nitric acid, and then several times with deionized water.

2.6. Image acquisition and analysis

Images were obtained using a Light Microscope DM1000 (Leica Microsystems, Germany) and a digital camera ICC50HD (Leica Microsystems, Switzerland). To determine *Chlorella* sp. size, cells were photographed and analyzed using the image software ImageJ (ImageJ, NIH, USA). From the light microscopy images cell volume was calculated using the measured diameters and by approximating the cells to a sphere using the formula given by Hillebrand [32]. For scanning electron microscopy (SEM) imaging cells were prepared using a standard glutaraldehyde fixation and ethanol dehydration protocol. Cells and particles were fixed in 2.5% glutaraldehyde in 0.1 M PBS buffer pH 7 and attached to a paper filter disk. Increasing concentrations of ethanol starting from 50% to 100% were used to dehydrate the cells on the disk. The filter disk was coated with a thin gold layer prior to imaging with a microscope Inspect S50 (FEI, The Netherland) combined with an energy dispersive X-ray analyzer (EDS) EDAX Octane Pro (Panalitical, The Netherland).

2.7. Fourier Transform Infrared (FT-IR) measurements and analysis

FT-IR spectra were collected in a UATR Spectrum Two spectrometer (Perkin-Elmer, United Kingdom) in the range of 600–3000 cm^{-1}. The samples were conditioned as following: the algae in the culture medium were centrifuged at 5000*g* during 10 min. Supernatants were removed and the pellets were washed with deionized water and centrifuged again in similar conditions. The pellets with the algae cells were placed over the crystal of the UATR dried with nitrogen flow and the measurements were performed by applying a moderated pressure over the dried sample, using a similar pressure in all measurements. Special attention was made to a complete cover of all the crystal with the sample. Algae without the exposure to Zn^{2+} (control), and exposed to Zn^{2+} concentrations of 25, 50, 75, 100 and 125 mg/L were measured. The absorption difference spectra were calculated directly with the Perkin Elmer's software, without any correction of the intensity, using as subtracting reference data the spectrum without Zn exposure (control). Peaks corresponding to the different functional groups assignment and identification were done following references from the literature [33,34].

2.8. Statistical treatment

All experiments were performed as minimum in triplicates. Statistical treatment and significant differences were evaluated either by one way ANOVA with Sidak's multiple comparisons test or unpaired *t*-test with Welch's correction that does not assume variance homogeneity. Statistical analysis was performed using Prism (GraphPad Software, USA). In all cases the significance level was set at $p = 0.05$. Extra details on statistical treatments are indicated in the figures captions or tables footnotes.

3. Results and discussion

3.1. Magnetic particles and Chlorella sp. cells characterization

Harvesting assays were performed using two different materials: 1) IOPs obtained by the co-precipitation method, and 2) NMC. For material characterization, and to evaluate its usage in cells harvesting, XRD, ζ-potential by DLS and magnetization analysis were performed. Characterization studies results are summarized in Fig. 1 in addition Appendix A shows SEM images of the magnetic particles (Supplementary Fig. A 1). In both samples, XRD profiles evidence predominance of ferrite phase, with broad lines characteristic of the presence of a nanocrystalline morphology. In addition, the XRD patterns of IOPs and NMC particles display six broad peaks at $2\theta = 30.1$, 35.6, 43.4, 53.6, 57.2, and 62.8° consistent with a spinel structure and would indicate the presence of maghemite (γ-Fe_2O_3) and/or magnetite (Fe_3O_4) iron phases according to the respective powder diffraction file (PDF) numbers of 39–1346 and 19–0629. The DLS analysis gave a hydrodynamic mean size around 236 nm for IOPs in water suspension and a positive ζ-potential of 11 mV. In addition, a low saturation magnetization $M_S = 4$ emu/g with no hysteresis was determined for these particles. Low magnetization, absence of hysteresis and the linear magnetic behavior in the higher field region apparently indicates a higher level of oxidation with respect to the ferrite. These values were obtained by measuring the raw material with no processing and/or functionalization of the IOPs. On the other hand, NMC showed, after ball-milling, a mean particle size of around 225 nm in water suspension with a broad size distribution, negative ζ-potential of −23.4 mV, a magnetization of $M_S = 42$ emu/g and coercive field of $H_C \sim 200$ Oe. In both particles, IOPs and NMC, the broad peaks in the XRD profiles indicate a lower crystalline size when compared to the particle hydrodynamic diameter measured by DLS, probably consequence of agglomeration and/or polycrystalline morphology of the particles. Since a net negative charge would not allow cell-particles interaction, surface charge of the NMC particles was modified by polyethylenimine functionalization (NMCP). The binding of the polymer changed the ζ-potential from −23 mV to 50 mV, increased particles size to around 315 nm, but did not affect magnetic properties (data not shown). The NMC and NMCP samples presented higher saturation and coercivity when compared to the IOPs. However, it is worth mentioning that the milling procedure and the natural origin of the sample (with impurities) lead to an expected reduction in the magnetization with respect to the natural clay before ball milling. This is a consequence of the stress and defects produced by the physical process. Nevertheless, magnetization was several times higher than for IOPs.

The *Chlorella* sp. cells had a spherical morphology and a cell diameter ranging from 2.5 to-7 μm. The strain cultures show no tendency to cell aggregation or biofilm formation and presented very high cell density ($> 90 \times 10^6$ cells/mL) (Supplementary Fig. A 2 panel A and B). The ζ-potential measurements showed negative values of −30.2 and − 32.8 for exponential and stationary cells respectively. Finally, electron microscopy (SEM) images showed an irregular cell surface, covered with prominences that could contribute to increase the adsorption area (Supplementary Fig. A 2 panel C).

3.2. Chlorella sp cells harvesting using low cost magnetic particles

Harvesting efficiency was thoroughly tested for both characterized materials, IOPs and NMC. The assays were performed as described in the materials and methods section and different forms of the NMC (bare and functionalized) were tested. Since cell surface functional groups could change with the physiological state of the cultures and, therefore, cell-particles interaction could be affected, harvesting experiments were carried out at exponential and stationary growth phases. Given the fact that IOPs showed lower magnetization properties, the amount of particles used in these assays was set up based on the IOPs harvesting performance. This amount was tested in a previous assay in order to achieve ≥90% harvesting efficiency for 9×10^6 cells/mL (data not shown). Table 1 shows harvesting efficiencies at different growth phases using IOPs, NMC and NMCP particles. These experiments showed a harvesting efficiency of > 90% for both particles, the IOPs and NMCP. A macro- and microscopic view of the harvesting assays as wells as cell surface- particles interaction are shown in supplementary Fig. A3 and A4 (Appendix A). As it was stated before, the positive charge of particles neutralized, and therefore attach to, the negatively charged algal cells (Supplementary Fig. A5).

One of the main objectives of the present study was to determine the efficiency of using low cost and non-contaminant magnetic material for algae biomass harvesting. Different types of IOPs have been successfully applied for algae harvesting [14,15] but to our knowledge, it is the first time that NMC is used for algae recovery. Another key issue analyzed in

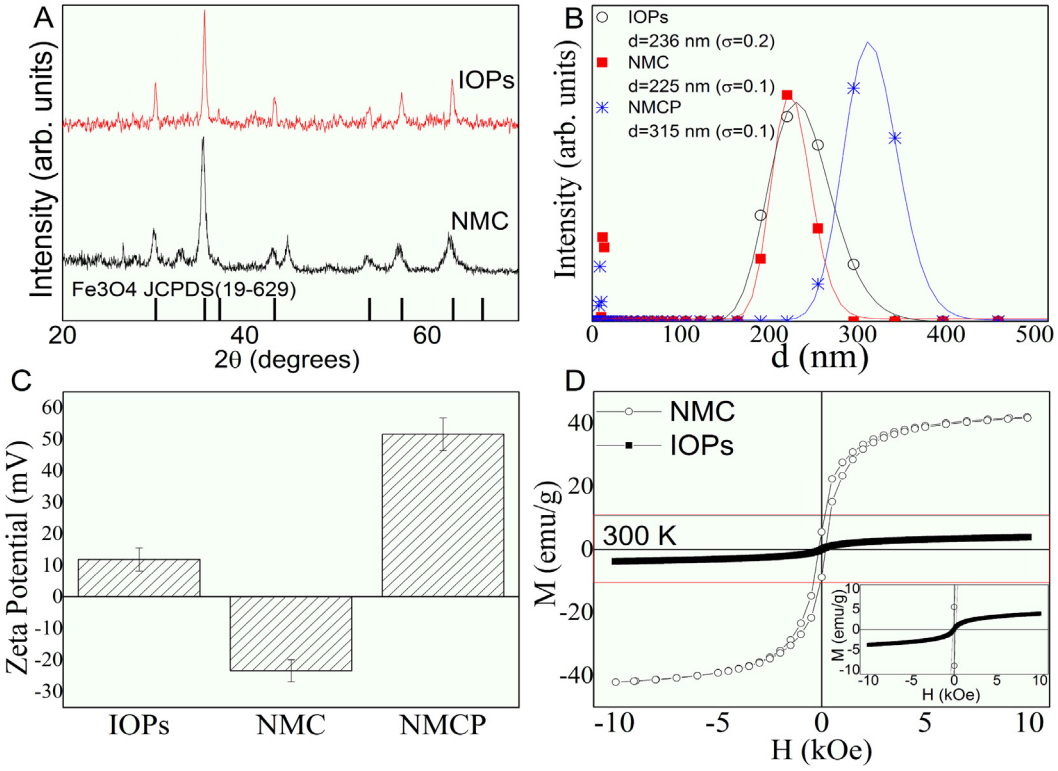

Fig. 1. Particles characterization. A. XRD pattern of the magnetic material, B. Dynamic Light scattering analysis. C. ζ-potential measurements of the different magnetic particles in deionized water (pH = 7.0). D. Magnetization analysis of the Iron Oxide Particles (IOPs), Natural Magnetic Clay (NMC) and Natural Magnetic Clay -Polyethylenimine (NMCP) particles. Arb. Units: arbitrary units; d: diameter; nm: nanometers; σ: standard deviation; mV: milivolts; M: material magnetization (emu/g); H: External applied field (kOe). (This is a 2 column fitting image, color: online only).

this work, was regarding the effect of the physiological state of the algae cultures on the harvesting process. It has been reported that surface functional groups tend to change during culture progression [19,35,36] and this could impact on metal ion removal and on the magnetic harvesting. *Chlorella* sp. cells harvesting in exponential and stationary phase with IOPs, naked NMC and NMCP was analyzed. Harvesting efficiencies were around 95% for IOPs and NMCP, but were negligible for naked NMC (Table 1). This could be explained by the ζ-potential differences (Fig. 1C). In an environment with low ionic strength, the interaction between fresh water algal cells and particles is mainly due to electrostatic attraction [37]. Supplementary data (Fig. A 5) shows a detailed of the cell surface functional groups that contribute to the net negative charge of the cells and the chemical groups that, depending on the pH, positively charge the particles. Algal cells as well as the naked NMC particles showed a net negative charge, which explains why the harvesting assay did not work. On the other hand, IOPs and NMCP particles had positive charge at the working pH and allowed cells particles interaction and high separation efficiencies. Prochazkova and coworkers reported that, although ζ-potential change, *C. vulgaris* maintains a negative charge even at very low pH [15]. Contrary to this, the IOPs, constituted mainly by metal oxides such as Fe_3O_4 and/or γ-Fe_2O_3, are covered by hydroxyl species and have a pH-sensitive surface charge that becomes positive below the isoelectric point which is 7.9 ± 0.2 [13,18]. In order to obtain higher harvesting efficiencies regardless of environmental changes particles with functional coating have been engineered [38,39]. This allowed magnetic separation of negative ζ-potential algae with positive ζ-potential particles by electrostatic attraction, irrespective of the original particles surface charge. Regarding the effect of the growth phase of the culture on the harvesting, there were no differences in the efficiency of the assay for exponential and stationary cultures. This could be explained by the fact that cell surface charge and the ζ-potential were negative and similar in

Table 1
Harvesting efficiencies of *Chlorella* sp. biomass with different types of magnetic particles. The table summarizes the harvesting performance for different types of particles applied to the two growth phases of the cultures, exponential and stationary. Zeta potential of the cells and particles are indicated in the table. M: mean; STD: Standard Deviation; IOPs: Iron Oxide Particles; NMCP: Natural Magnetic Clay- Polyethylenimine. Harvesting assays for the different material were done in triplicates and in three individual experiments.

Harvesting efficiency						
	Culture condition					
Magnetic particles	Exponential (ζ-potential: −30.2 ± 5.05)		Stationary (ζ-potential: −32.8 ± 5.31)		ζ-potential of the particles	
	Mean (%)	STD	Mean (%)	STD	Mean	STD
IOPs (30 mg)	95.7	± 3.1	94.3	± 2.1	11.9	3.7
NMC (30 mg)	4.0	± 6.9	–	–	−23.4	3.5
NMCP (30 mg)	97.7	± 0.6	94.3	± 3.1	51.6	5.2
NMCP (15 mg)	90.0	± 6.4	–	–		

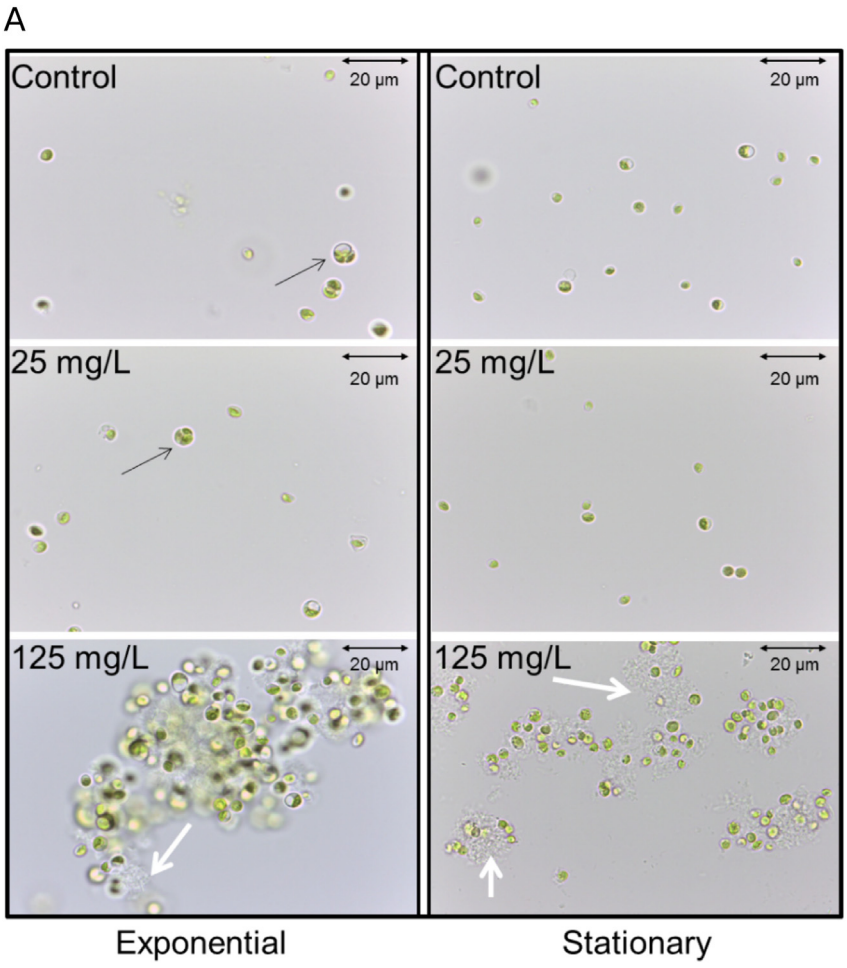

Fig. 2. Metal exposure effect on *Chlorella* sp. morphology and cell size. A. Images of exponential (*E*-phase) and stationary (S phase) cell cultures exposed to, 0, 25 and 125 mg/L of Zn^{2+} under 1000 magnification. Black arrows indicate the presence of tetraspores in the exponential cultures while white ones outline the secreted mucilage that is evident at 125 mg/L. B. Effect of Zn^{2+}, 25 and 125 mg/L in cell size (volume) of exponential and stationary *Chlorella* sp. cultures. Statistical analysis was done with one way ANOVA with Sidak's multiple comparisons test ($n = 123$). The significance level was set at 0.05, being $*p < 0.05$ in all cases. (This is a 1.5 to 2 column fitting image, color: online only).

both states. It is worth mentioning that, although the two types of particles worked within the first 5 min of the assay the NMCP particles harvested > 95% of the cells in < 2 min, while for IOPs it took 5 min to reach similar results. In the present study, harvesting experiments were performed using the same mass of each type of particles in order to be able to compare the results. However, considering the differences on particles magnetization, a reduced amount of NMCP was tested on cell harvesting. It was found that 15 mg harvested 90% of the cells (Table 1). From this result, it can be concluded that it is possible to get similar harvesting efficiencies by reducing the amount of NMCP particles. This is an important practical aspect when considering future magnetic-assisted treatments of contaminated wastewater.

3.3. Effects of zinc exposure on cell morphology and surface properties

3.3.1. Cell cultures and cell size

To evaluate the effect of the zinc treatment, the overall culture aspect and cell morphology on exponential and stationary phase was first analyzed. The most remarkable effect of the Zn^{2+} was the presence of a mucilage that was only present in the 125 mg/L of Zn^{2+} treatments

(Fig. 2A). Under the microscope exponential cultures showed clear signs of cell proliferation in control and 25 mg/L of Zn^{2+}, while there were no signs of this on the 125 mg/L of Zn^{2+} treatment. The stationary cultures showed no cell proliferation at all (Fig. 2A). Treatments within the same culture condition showed no differences in size. However, control and Zn^{2+} treated cells in the stationary phase presented a reduction in cell size when compared to the exponential ones. The cell volume for the different growth phases and Zn^{2+} treatments are shown in Fig. 2B. These results indicate a tendency in the reduction of the cell size due to the age of culture and to metal exposure (Fig. 2A and B). In agreement, Pereira and coworkers reported that a Cr^{+3}tolerant *Dictyosphaerium chlorelloides* showed a decrease in cell size and a change in cell morphology upon Cr^{+3} exposure [40]. Mucilage secretion happened in both growth phases in response to high Zn^{2+} concentration. Although, it is possible that part of the mucilage was being released to the media and going into the solution, live images under light microscopy showed that it was associated to the cell surface (Fig. 2A). Therefore, it can be proposed that the secretion of this polymer is a cellular mechanism to alleviate metal toxicity. This idea is supported by published studies that propose that extracellular polysaccharides act as natural metal chelators [41,42]. The secreted mucilage in response to Zn^{2+} could be composed mainly by polysaccharide with high phosphorous content as already reported in some *Chlorella* species [41]. Mucilage composition was also inferred by FT-IR and EDS analysis. These results are presented and discussed in the next section.

3.3.2. Cell morphology and cell surface analysis

Algal cells treated with Zn^{2+} were analyzed by SEM. Fig. 3 shows pictures of the control and Zn^{2+} treatments (125 mg/L) in exponential and stationary cells. In the zinc treated cultures, a material deposition that looked like small spheres of a nanometric size was observed (Fig. 3A c & d bottom panels, white arrows). These were more prominent in the exponential treated cultures than in the stationary ones. Another manifestation of the mucilage deposition was a continuous layer surrounding the cells or groups of cells that were similar in both growth phases (Fig. 3A c & d upper panel, white asterisks). Energy dispersive spectroscopy (EDS) analysis on treated cultures showed that the deposited material had an increase in zinc and phosphorus abundance respect to the control cells in which zinc was not detectable (data not shown). Since metal adsorption might affect surface charge, ζ-potential measurements were performed. Fig. 3B shows the potential measured for the different growth phases during Zn^{2+} treatment at a pH of 5.5. Although, the addition of Zn^{2+} to the growing media showed a tendency to reduce the negative cell surface charge, the differences were not significant and the net charge remained negative.

In order to characterize the role of cell surface functional groups during Zn^{2+} treatment and to evaluate possible metal complexation sites, FT-IR analysis was performed. To obtain a detailed description of the changes caused by zinc exposure, cell culture samples exposed to different Zn^{2+} concentrations (25, 50, 75, 100 and 125 mg/L) were analyzed. Differences among exponential and stationary cultures were also evaluated. The results of these experiments are shown on Fig. 4. Panel A spectrum shows the main analyzed bands in this study. The FT-IR analysis of the exponential and stationary phases showed no differences in the functional groups present on the cell surface. Nevertheless, all of them, except for the phosphates and polysaccharides, were more abundant in the exponential phase (Fig. 4A). In the exponential cultures, the groups were independent of Zn^{2+} concentration, meaning that the observed spectrum for the 25 mg/L dose was very similar to the 125 mg/L one. The spectrum for the exponential phase showed, when compared to the control, an increase of the ν(C═O) and δ(N−H) (amide I and II, bands 1650 cm^{-1} and 1540 cm^{-1}) from the amide functional

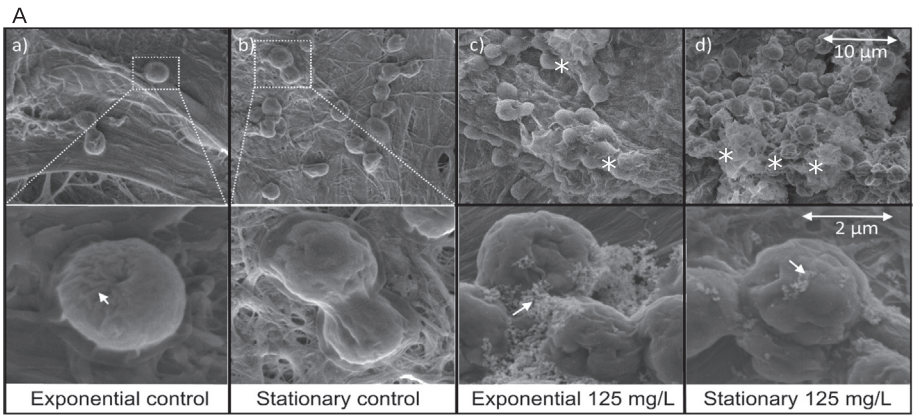

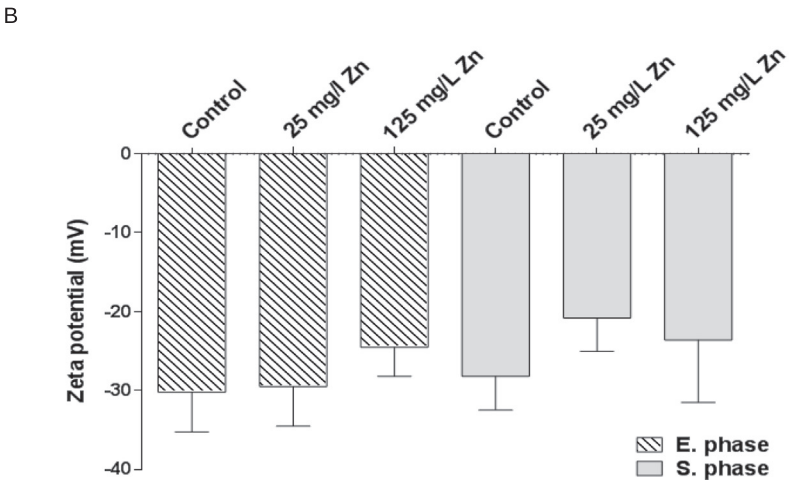

Fig. 3. Effect of Zn^{2+} on cell surface and morphology. A. SEM images of exponential (*E*-phase) and stationary (S-phase) cultures exposed to 0 (a and b) and 125 mg/L of Zn^{2+} (c and d). Upper and bottom panels in a and b shows the general morphology of the control cells (10,000 magnification). Panels in c and d show a detailed of the cells and deposited material induced by Zn^{2+} treatment (white arrows in the bottom panels and white asterisks in the upper ones). B. Graph of the ζ-potential measurements of control and Zn^{2+} treated cultures at the exponential (E) and stationary (S) growth phase in culture medium (pH = 5.5). Zeta potential measurements were done one time by triplicates.

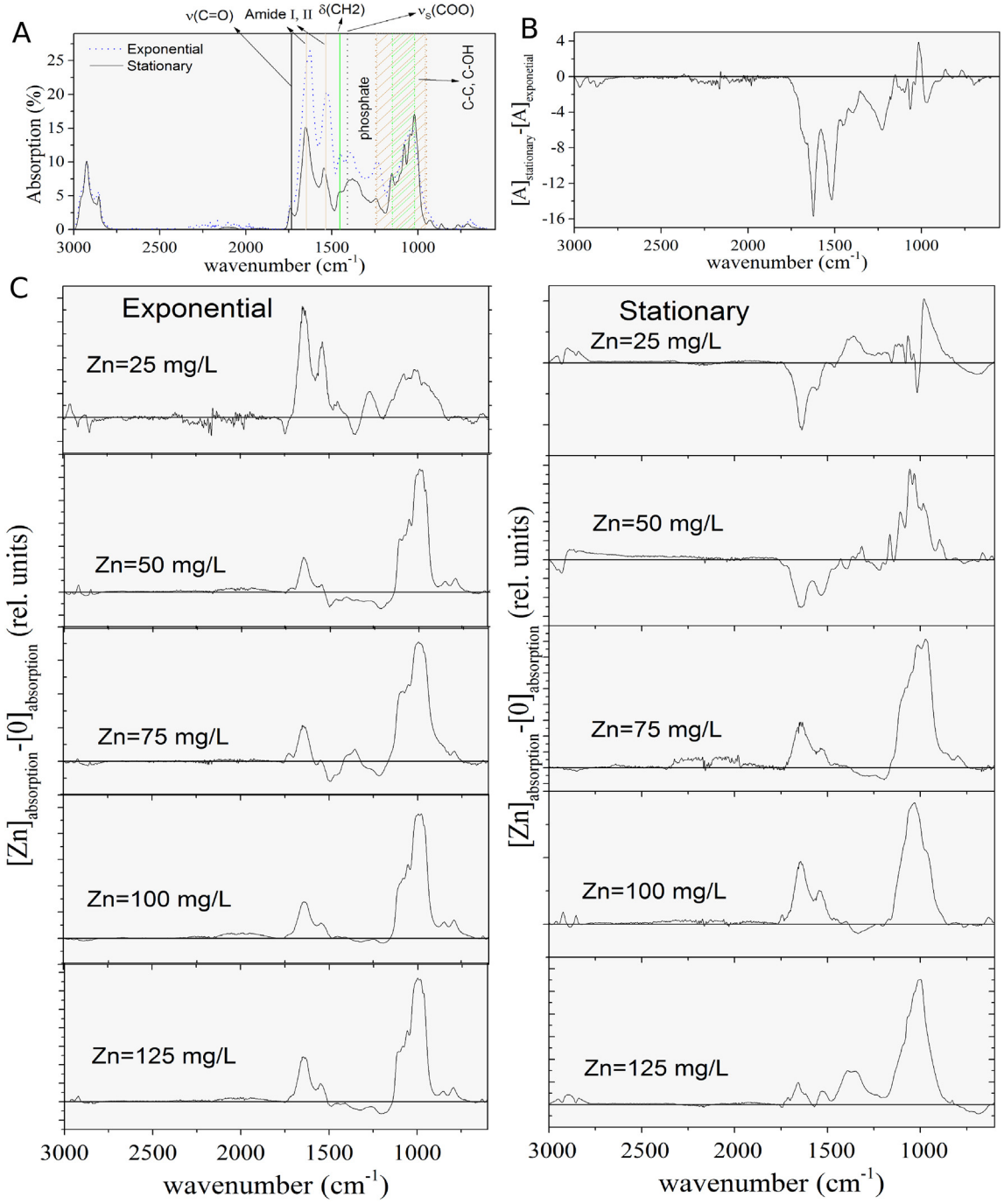

Fig. 4. Cell surface functional groups rearrangements during Zn^{2+} treatment. A. Infrared spectra of exponential and stationary growth phases of *Chlorella* sp. cultures (control, no Zn^{2+}), the identified bands were: 1650 $cm^{-1}\nu$(C═O) corresponding to lipids, corresponding to amide I, 1540 $cm^{-1}\delta$(N−H), corresponding to amide II, ~1455 $cm^{-1}\delta(CH_2)$, ~1398 $cm^{-1}\nu_s$(COO) all corresponding to proteins, and bands between 1254 and 900 $cm^{-1}\nu_{as}$(P═O), ν_s(P═O), C−C and C−OH corresponding to phosphates and polysaccharides. B. Differences in the infrared spectra of exponential and stationary states of the control cultures. C. *Chlorella* sp. cultures treated with increasing Zn^{2+} concentration ranging from 0 to 125 mg/L. The spectra were obtained by doing the difference between the treatments and the control (0 mg/L of Zn^{2+}). Peaks intensities are expressed in relative unit.

groups that belong to the proteins present in the cell wall [34] (Fig. 4C, left panel). These groups did not appear in the stationary phase at the 25 and 50 mg/L of Zn^{2+} treatments. However, they showed up in the 75 and 100 mg/L ones, to finally decrease at the 125 mg/L (Fig. 4C, right panel). A second change was observed on the bands between 1245 cm^{-1} and 900 cm^{-1}corresponding to symmetric and asymmetric stretching vibration of the phosphates and the C−C and C−OH from polysaccharides (1150–1020 cm^{-1} range). Since phosphates and polysaccharides contribute to bands between 1150 and 1020 range, exact band assignment is complicated in this region of the absorption spectra. Cells in the exponential and stationary growth phase showed an increase on these bands in the presence of Zn^{2+}, indicating that the groups are involved in metal complexation. Again, similarly to the amide groups, this response occurred first in the exponential cultures (at 25 mg/L) and later on the stationary ones (Fig. 4C, right panel).

Cell surface functional groups associated with polysaccharides and proteins [4,28] play an important role in determining cell surface charge. In order to evaluate the effect of zinc, changes in cell surface

charge and functional groups involved in metal binding were analyzed. The ζ-potential measurements showed that although the charge turned less negative (from −32 to −20 mV), *Chlorella* sp. cells maintained a net negative surface charge after the metal adsorption process. By FT-IR analysis the role of functional groups on metal binding was identified. Measurable changes in the spectrum during metal treatment represent functional groups complexation with metals. This allows to map metal-functional groups interaction, as well as an increase or decrease of the involved groups [34]. The study of the position and intensity of the main IR bands, and their modification following metal exposure and adsorption, provides useful information on the chemical groups involved in metal ions binding [43–45]. By FT-IR analysis, it was found that amide, phosphate and polysaccharides groups are involved in the Zn^{2+} coordination and complexation by *Chlorella*. This partially agrees with the reported coordination of uranium by active *Chlorella* cells, performed mainly by carboxylic and phosphate groups [34]. The *Chlorella* sp. cells analyzed in this study showed a similar behavior to the ones described for uranium by Vogel [34]. An analysis of groups involved in the coordination of Ni^{2+}, Zn^{2+} and Pb^{2+} by *Arthrospira platensis* and *C. vulgaris* showed that carboxylic groups were mainly involved in coordination and ionic exchange of bivalent ions, but also electron donor groups, such as amino, amide and hydroxyl groups were likely to play a role in the adsorption process [46]. Finally, it is worth to mention that energy dispersive spectroscopy and FT-IR analysis support the hypothesis of mucilage secretion as a response to Zn^{2+} treatments and that one of the main components are the polysaccharides. Mucilage secretion and deposition on cells surface (Figs. 2 and 3) correlates with an increase in phosphates groups as well as polysaccharides bands detected by FT-IR during Zn^{2+} treatments (Fig. 4C, 1245–900 cm^{-1} range). Along with this, energy dispersive spectroscopy analysis showed an enrichment of zinc and phosphorous on the treated cells when compared to the control.

3.4. Zinc removal is compatible with magnetic particles harvesting

Metal removal efficiency by algae was analyzed before and after harvesting in order to determine the effect of magnetic particles on remediation efficiency. Additionally, magnetic harvesting was analyzed after metal removal to evaluate possible effects of metal remediation on the recovery efficiency. Regarding to zinc removal, a remediation efficiency of > 60% for 25 mg/L of Zn^{2+} treatments over a period of 24 h was found (Table 2). Furthermore, experiments showed that *Chlorella* sp. cells exposed to 25 mg/L of Zn^{2+} were perfectly harvested by both magnetic materials, reaching a harvesting efficiency higher than 96% in all cases (Table 3). The harvesting with IOPs produced an increase of the zinc concentration in the supernatant, when comparing metal removal efficiency before and after the harvesting. The increase was statistically significant in the exponential and stationary cultures (see Table 2, footnotes a and b). On the other hand, when the NMCP were used in the harvesting, a decrease in the final Zn^{2+} concentration was observed. The reduction was significant for the exponential phase and the net effect was an increase on metal removal efficiency by the formed system (see Table 2, footnote c). As the algal recovery with the NMCP had no negative effect on metal remediation it was tested if at higher doses, remediation and magnetic harvesting were compatible. Also, metal adsorption by NMCP alone was tested. Algal cells in exponential and stationary growth phase were exposed to 125 mg/L of Zn^{2+} and harvested as described before. The recovery efficiency reached > 95% at high metal dose in both growth phases (Table 3). Regarding metal removal, there was a clear difference in both conditions, exponential culture adsorbed > 40% of the Zn^{2+} added, while the stationary one only removed 15% of the Zn^{2+} over a period of 24 h (Table 2). These results clearly showed that at high Zn^{2+} doses the exponential culture performed better for metal remediation.

Given the fact that algae harvesting is one of the most cost-consumption step in their industrial application, new cost-effective techniques are needed. Among them, magnetic harvesting offers the advantages of easy operation, short time consumption and low energy requirements. There has been widespread research in improving particles recovery to reduce even more the cost of this technique [16,47–49] However, in the case of applying magnetic harvesting for algae employed in metal remediation, the re-use of the particles should be carefully analyzed. Strategies to recover particles, but not to release the metals adsorbed in the algal biomass, should be developed.

Table 3
Harvesting efficiencies after zinc removal. The table summarized the results of biomass harvesting experiments after metal removal. M: mean; STD: Standard Deviation; IOPs: Iron Oxide Particles; NMCP: Natural Magnetic Clay-Polyethylenimine. Harvesting assays where performed by triplicate.

Harvesting efficiency during zinc removal				
	Culture condition			
	Exponential		Stationary	
Zn^{2+} dose	M (%)	STD	M (%)	STD
IOPs/Zn^{2+} (25 mg/L)	97.5	± 0.71	97.5	± 2.12
NMCP/Zn^{2+} (25 mg/L)	97	± 2.82	98	± 2.82
NMCP/Zn^{2+} (125 mg/L)	98.7	± 0.6	98.3	± 0.6

Table 2
Zinc removal efficiencies and its compatibility with magnetic harvesting. The table summarized the metal removal efficiencies before and after the harvesting with the different utilized magnetic materials. Statistical analysis was done applying an unpaired *t*-test with Welch's correction and the significance level was set at 0.05. The analyzed pairs and its grade of significance are indicated in the table. Only significant differences are shown. M: mean; STD: Standard Deviation; IOPs: Iron Oxide Particles; NMCP: Natural Magnetic Clay- Polyethylenimine. Metal removal assays were done at two different doses, by triplicates one time.

Removal efficiency before harvesting					Removal efficiency after harvesting							
	Culture condition				Culture condition							
	Exponential		Stationary		Exponential				Stationary			
					IOPs		NMCP		IOPs		NMCP	
Zn^{2+} dose	M (%)	STD	M (%)	STD	M (%)	STD	M (%)	STD	M (%)	STD	M (%)	STD
25 mg/L	66.4[a,c]	± 11.2	80.4[b]	± 10.0	41.6[a]	8.0	86.4[c]	± 8.8	35.9[b]	3.7	86.5	± 0.9
125 mg/L	44.8	± 9.9	15.3[d]	± 7.5	–	–	63.4	± 11.2	–	–	47.8[d]	± 5.3

[a] Exponential vs exponential-IOPs $^{*}p = 0.0124$.
[b] Stationary vs stationary-IOPs $^{****}p = 0.0001$.
[c] Exponential vs exponential-NMCP $^{*}p = 0.0355$.
[d] Stationary vs stationary-NMCP $^{**}p = 0.0051$.

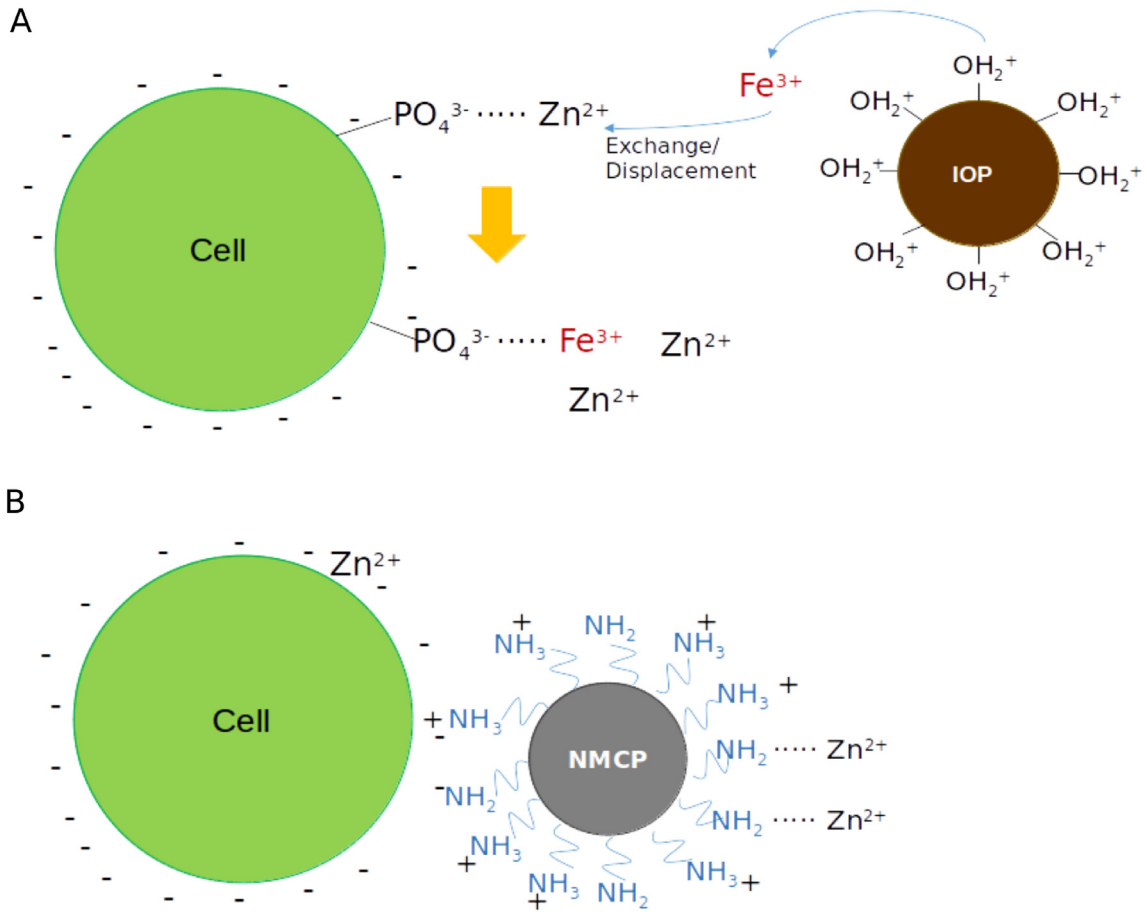

Fig. 5. Metal removal and magnetic harvesting coupled processes. A. Possible scenario to explain the displacement of zinc observed during the harvesting with IOPs. The scheme shows the proposed mechanism by which the leached Fe^{3+} ions compete with Zn^{2+} for the phosphates binding site producing the exchange on the cell surface. B. NMCP particles - cells interaction as well as the Zn^{2+} interactions with the amine groups of the functionalized particles. IOP: Iron Oxide Particles; NMCP: Natural Magnetic Clay-Polyethyleneimine (This is a 2 column fitting image, color: online only).

Cultures at different growth phases were perfectly harvested after exposure and metal removal. This implicates that, although the metal treatments induced mucilage secretion and changes in the abundance of some of the surface functional groups, these effects did not impact negatively on harvesting efficiency. These results are consistent with the fact that ζ-potential, which is probably the main factor governing cells-particles interaction, did not changed significantly. The ζ-potential of the cells remained negative even at high doses of Zn^{2+}. Although metal chelation by the cell wall groups could reduce the negative charges from the surface, it was seen that cells compensate by increasing the abundance of negatively charged groups (as observed by FT-IR analysis). Taken together all this data proved one of the main objectives of this work, the compatibility of metal removal with magnetic harvesting. Regarding metal removal for 25 mg/L Zn^{2+}, results presented here are in good agreement with those reported for Zn^{2+} remediation by *C. vulgaris* [50]. Interestingly when the initial Zn^{2+} concentration was higher, 125 mg/L, the efficiency of metal removal of the exponential culture was almost 45%, against 15% for the stationary one (Table 2). Cells in stationary phase showed less capacity to remove the Zn^{2+} at high concentrations. In the FT-IR analysis it was observed that, although cells in the stationary phase were capable of exposing polysaccharides, they showed a lower capacity to expose amide and phosphate groups when compared to the exponential ones at low doses (25 and 50 mg/L Zn^{2+}). This situation would reduce the potential sites for metal chelation and this could explain the differences observed in the removal efficiencies at the higher dose. Li and coworkers observed that for *Chlorella* sp. QB-102 most of the adsorption of Pb^{2+} occurred during the initial period of the stationary phase [36]. Conversely, in the present work results showed that at high Zn^{2+} concentration cultures in the exponential phase performed better metal removal. It is worth to notice that this study analyzed remediation with live algae, meanwhile Li and coworkers [36] employed dead algal biomass and a different metal, Pb^{2+} instead of Zn^{2+}.

As particles interact with the cell surface, it was analyzed if the particle-cell interaction had an effect on the adsorbed metal stability and consequently on the remediation process efficiency. Compatibility among magnetic separation and metal remediation by algae showed clear differences between both types of particles. After the harvesting with IOPs there was an increase in the Zn^{2+} concentration in the supernatant that took metal remediation efficiency to < 45% in the stationary cultures (Table 2, 25 mg/L of Zn^{2+} dose). This result indicates that there was a displacement of part of the Zn^{2+} that was originally adsorbed to the algal cell wall. The Zn^{2+} displacement that occurred during the harvesting with IOPs could be attributed to leached iron species originated from the IOPs. It is well known that at acidic conditions iron oxide-based materials without a protective coating layer can undergo dissolution and release iron ions in a process called leaching [51]. The FT-IR analysis showed that phosphate is one of the functional groups that change the most in response to the presence of Zn^{2+}, suggesting that it is a good candidate for binding the metal. Considering the affinity of cations, such as Zn^{2+} and $Fe^{2+/3+}$, for PO_4^{-2} [52], the increase of Zn^{2+} after the harvesting with IOPs could be due to a competition of both metals for the same adsorption sites. Fig. 5 A shows a schematic view of the hypothesis and proposed scenario. As it was said before, the harvesting with NMCP produced a reduction of the remaining Zn^{2+} in the medium, when 125 mg/L dose

was applied, that took metal removal from 15 to > 45% on the stationary cultures (Table 2). This is probably due to a Zn^{2+} complexation by the amino groups present in the PEI of the NMCP. Fig. 5B shows a schematic view of the proposed interaction. Martin and collaborators work [53] supports this explanation. The authors reported > 90% of Zn^{2+} removal from aqueous solution, at neutral pH and at 10 mg/L Zn^{2+} initial concentration, by aminopropyl modified absorbent material rich in amino groups. [53]. The experiments done in this research showed that the NMCP resulted in high algal harvesting efficiency, were compatible with metal remediation performed by algae and also improved the metal remediation efficiency (Tables 1, 2 and 3).

4. Conclusion

This paper makes a novel contribution in the field of magnetic cell separation and metal remediation using low cost magnetic material and showing the compatibility of the processes. Cells metal treatments had a minor effect on cell surface charge, due to a compensation mechanism in which negatively charged groups increase. Both tested magnetic materials showed comparable and very good performance on biomass harvesting. The harvesting with the IOPs affected the metal removal efficiency. Conversely, the harvesting with the NMCP improved the remediation efficiency. Physiological state of the cultures had no effect on harvesting process although showed significant differences on metal removal efficiencies.

Contributions

C·B conceived the idea. GF and CB designed and analyzed the experiments. GF, RT, DC EL MM NF carried out the experiments. CB and GF wrote the manuscript DP and RZ made critical revisions on the article for important intellectual content. All authors reviewed and approved the final manuscript.

Acknowledgements

Special thanks to the Staff of the INVAP's SE Chemistry Laboratory for the contributions with the metal determination by ICP OES. Also we want to thanks Mrs. Paula Troyon from the Characterization Materials Department (CNEA) for the SEM photography and EDS analysis performed with Fei Inspect S50 and EDAX Octane Pro.

Declaration of interest

None.

Funding

This study was partially supported by the National Atomic Energy Commission (CNEA) and National Scientific and Technical Research Council (CONICET).

Consent statement

No conflicts, informed consent, human or animal rights applicable.

Appendix A. Supplementary data

Supplementary data to this article can be found online at https://doi.org/10.1016/j.algal.2018.05.022.

References

[1] A. Singh, P.S. Nigam, J.D. Murphy, Renewable fuels from algae: an answer to debatable land based fuels, Bioresour. Technol. 102 (2011) 10–16, http://dx.doi.org/10.1016/j.biortech.2010.06.032.

[2] L. Christenson, R. Sims, Production and harvesting of microalgae for wastewater treatment, biofuels, and bioproducts, Biotechnol. Adv. 29 (2011) 686–702, http://dx.doi.org/10.1016/j.biotechadv.2011.05.015.

[3] C.M. Monteiro, P.M.L. Castro, F.X. Malcata, Metal uptake by microalgae: underlying mechanisms and practical applications, Biotechnol. Prog. 28 (2012) 299–311, http://dx.doi.org/10.1002/btpr.1504.

[4] K. Suresh Kumar, H.-U. Dahms, E.-J. Won, J.-S. Lee, K.-H. Shin, Microalgae – a promising tool for heavy metal remediation, Ecotoxicol. Environ. Saf. 113 (2015) 329–352, http://dx.doi.org/10.1016/j.ecoenv.2014.12.019.

[5] B. dos S.A.F. Brasil, F.G. de Siqueira, T.F.C. Salum, C.M. Zanette, M.R. Spier, Microalgae and cyanobacteria as enzyme biofactories, Algal Res. 25 (2017) 76–89, http://dx.doi.org/10.1016/j.algal.2017.04.035.

[6] Y. Chisti, Biodiesel from microalgae, Biotechnol. Adv. (2007), http://dx.doi.org/10.1016/j.biotechadv.2007.02.001.

[7] I. Anastopoulos, G.Z. Kyzas, Progress in batch biosorption of heavy metals onto algae, J. Mol. Liq. (2015), http://dx.doi.org/10.1016/j.molliq.2015.05.023.

[8] D. Vandamme, I. Foubert, K. Muylaert, Flocculation as a low-cost method for harvesting microalgae for bulk biomass production, Trends Biotechnol. 31 (2013) 233–239, http://dx.doi.org/10.1016/j.tibtech.2012.12.005.

[9] C.Y. Chen, K.L. Yeh, R. Aisyah, D.J. Lee, J.S. Chang, Cultivation, photobioreactor design and harvesting of microalgae for biodiesel production: a critical review, Bioresour. Technol. 102 (2011) 71–81, http://dx.doi.org/10.1016/j.biortech.2010.06.159.

[10] J.E. Coons, D.M. Kalb, T. Dale, B.L. Marrone, Getting to low-cost algal biofuels: a monograph on conventional and cutting-edge harvesting and extraction technologies, Algal Res. 6 (2014) 250–270, http://dx.doi.org/10.1016/j.algal.2014.08.005.

[11] N. Uduman, Y. Qi, M.K. Danquah, G.M. Forde, A. Hoadley, Dewatering of microalgal cultures: a major bottleneck to algae-based fuels, J. Renew. Sustain. Energy. 2 (2010), http://dx.doi.org/10.1063/1.3294480.

[12] S. Cheruvu, S. Van Ginkel, X. Wei, X. Zhang, D. Steiner, S.H. Rego De Oliveira, C. Xu, L.H. Kalil Duarte, E. Salvi, Z. Hu, H.J. Lee, R. Gijon-Felix, Y. Chen, Algae harvesting, Membr. Technol. Biorefining, 2016, pp. 309–328, , http://dx.doi.org/10.1016/B978-0-08-100451-7.00013-X.

[13] L. Xu, C. Guo, F. Wang, S. Zheng, C.Z. Liu, A simple and rapid harvesting method for microalgae by in situ magnetic separation, Bioresour. Technol. 102 (2011) 10047–10051, http://dx.doi.org/10.1016/j.biortech.2011.08.021.

[14] M. Cerff, M. Morweiser, R. Dillschneider, A. Michel, K. Menzel, C. Posten, Harvesting fresh water and marine algae by magnetic separation: screening of separation parameters and high gradient magnetic filtration, Bioresour. Technol. 118 (2012) 289–295, http://dx.doi.org/10.1016/j.biortech.2012.05.020.

[15] G. Prochazkova, I. Safarik, T. Branyik, Harvesting microalgae with microwave synthesized magnetic microparticles, Bioresour. Technol. 130 (2013) 472–477, http://dx.doi.org/10.1016/j.biortech.2012.12.060.

[16] S.K. Wang, A.R. Stiles, C. Guo, C.Z. Liu, Harvesting microalgae by magnetic separation: a review, Algal Res. 9 (2015) 178–185, http://dx.doi.org/10.1016/j.algal.2015.03.005.

[17] Y.R. Hu, C. Guo, L. Xu, F. Wang, S.K. Wang, Z. Hu, C.Z. Liu, A magnetic separator for efficient microalgae harvesting, Bioresour. Technol. 158 (2014) 388–391, http://dx.doi.org/10.1016/j.biortech.2014.02.120.

[18] K. Lee, S.Y. Lee, R. Praveenkumar, B. Kim, J.Y. Seo, S.G. Jeon, J.G. Na, J.Y. Park, D.M. Kim, Y.K. Oh, Repeated use of stable magnetic flocculant for efficient harvest of oleaginous *Chlorella* sp, Bioresour. Technol. 167 (2014) 284–290, http://dx.doi.org/10.1016/j.biortech.2014.06.055.

[19] Y.R. Hu, F. Wang, S.K. Wang, C.Z. Liu, C. Guo, Efficient harvesting of marine microalgae Nannochloropsis maritima using magnetic nanoparticles, Bioresour. Technol. 138 (2013) 387–390, http://dx.doi.org/10.1016/j.biortech.2013.04.016.

[20] Y.R. Hu, C. Guo, F. Wang, S.K. Wang, F. Pan, C.Z. Liu, Improvement of microalgae harvesting by magnetic nanocomposites coated with polyethylenimine, Chem. Eng. J. 242 (2014) 341–347, http://dx.doi.org/10.1016/j.cej.2013.12.066.

[21] S. Matsuda, A.R. Durney, L. He, H. Mukaibo, Sedimentation-induced detachment of magnetite nanoparticles from microalgal flocs, Bioresour. Technol. 200 (2016) 914–920, http://dx.doi.org/10.1016/j.biortech.2015.11.006.

[22] Y.C. Lee, K. Lee, Y.K. Oh, Recent nanoparticle engineering advances in microalgal cultivation and harvesting processes of biodiesel production: a review, Bioresour. Technol. 184 (2015) 63–72, http://dx.doi.org/10.1016/j.biortech.2014.10.145.

[23] C.T. Yavuz, A. Prakash, J.T. Mayo, V.L. Colvin, Magnetic separations: from steel plants to biotechnology, Chem. Eng. Sci. 64 (2009) 2510–2521, http://dx.doi.org/10.1016/j.ces.2008.11.018.

[24] L. Borlido, A.M. Azevedo, A.C.A. Roque, M.R. Aires-Barros, Magnetic separations in biotechnology, Biotechnol. Adv. 31 (2013) 1374–1385, http://dx.doi.org/10.1016/j.biotechadv.2013.05.009.

[25] R. Senthilkumar, K. Vijayaraghavan, M. Thilakavathi, P.V.R. Iyer, M. Velan, Seaweeds for the remediation of wastewaters contaminated with zinc(II) ions, J. Hazard. Mater. 136 (2006) 791–799, http://dx.doi.org/10.1016/j.jhazmat.2006.01.014.

[26] R.S. Oliveira, J.C. Dodd, P.M.L. Castro, The mycorrhizal status of *Phragmites australis* in several polluted soils and sediments of an industrialised region of Northern Portugal, Mycorrhiza 10 (2001) 241–247, http://dx.doi.org/10.1007/s005720000087.

[27] M.T.S.D. Vasconcelos, H.M.F. Tavares, Atmospheric metal pollution (Cr, Cu, Fe, Mn, Ni, Pb and Zn) in Oporto city derived from results for low-volume aerosol samplers and for the moss Sphagnum auriculatum bioindicator, Sci. Total Environ. 212 (1998) 11–20, http://dx.doi.org/10.1016/S0048-9697(97)00322-7.

[28] S.K. Mehta, J.P. Gaur, Use of algae for removing heavy metal ions from wastewater: progress and prospects, Crit. Rev. Biotechnol. 25 (2005) 113–152, http://dx.doi.org/10.1080/07388550500248571.

[29] I. Anastopoulos, G.Z. Kyzas, Progress in batch biosorption of heavy metals onto algae, J. Mol. Liq. 209 (2015) 77–86, http://dx.doi.org/10.1016/j.molliq.2015.05.023.
[30] E. Romera, F. González, A. Ballester, M.L. Blázquez, J.A. Muñoz, Biosorption with algae: a statistical review, Crit. Rev. Biotechnol. 26 (2006) 223–235, http://dx.doi.org/10.1080/07388550600972153.
[31] D. Kaplan, Absorption and adsorption of heavy metals by microalgae, Handb. Microalgal Cult. Appl. Phycol. Biotechnol. (2013) 602–611, http://dx.doi.org/10.1002/9781118567166.ch32.
[32] H. Hillebrand, C.-D. Dürselen, D. Kirschtel, U. Pollingher, T. Zohary, Biovolume calculation for pelagic and benthic microalgae, J. Phycol. 35 (1999) 403–424, http://dx.doi.org/10.1046/j.1529-8817.1999.3520403.x.
[33] P. Heraud, B.R. Wood, J. Beardall, D. McNaughton, Probing the influence of the environment on microalgae using infrared and Raman spectroscopy, New Appr. Biomed. Spectrosc. (2007) 85–106, http://dx.doi.org/10.1021/bk-2007-0963.ch007.
[34] M. Vogel, A. Günther, A. Rossberg, B. Li, G. Bernhard, J. Raff, Biosorption of U(VI) by the green algae *Chlorella vulgaris* in dependence of pH value and cell activity, Sci. Total Environ. 409 (2010) 384–395, http://dx.doi.org/10.1016/j.scitotenv.2010.10.011.
[35] X. Zhang, P. Amendola, J.C. Hewson, M. Sommerfeld, Q. Hu, Influence of growth phase on harvesting of *Chlorella zofingiensis* by dissolved air flotation, Bioresour. Technol. 116 (2012) 477–484, http://dx.doi.org/10.1016/j.biortech.2012.04.002.
[36] Y. Li, L. Xia, R. Huang, C. Xia, S. Song, Algal biomass from the stable growth phase as a potential biosorbent for Pb(ii) removal from water, RSC Adv. 7 (2017) 34600–34608, http://dx.doi.org/10.1039/C7RA06749F.
[37] P.Y. Toh, B.W. Ng, A.L. Ahmad, D.C.J. Chieh, J. Lim, The role of particle-to-cell interactions in dictating nanoparticle aided magnetophoretic separation of microalgal cells, Nano 6 (2014) 12838–12848, http://dx.doi.org/10.1039/c4nr03121k.
[38] K. Lee, S.Y. Lee, J.G. Na, S.G. Jeon, R. Praveenkumar, D.M. Kim, W.S. Chang, Y.K. Oh, Magnetophoretic harvesting of oleaginous *Chlorella* sp. by using biocompatible chitosan/magnetic nanoparticle composites, Bioresour. Technol. 149 (2013) 575–578, http://dx.doi.org/10.1016/j.biortech.2013.09.074.
[39] P. Liu, T. Wang, Z. Yang, Y. Hong, Y. Hou, Long-chain poly-arginine functionalized porous Fe3O4 microspheres as magnetic flocculant for efficient harvesting of oleaginous microalgae, Algal Res. 27 (2017) 99–108, http://dx.doi.org/10.1016/j.algal.2017.08.025.
[40] M. Pereira, M.C. Bartolomé, S. Sánchez-Fortún, Bioadsorption and bioaccumulation of chromium trivalent in Cr(III)-tolerant microalgae: a mechanisms for chromium resistance, Chemosphere 93 (2013) 1057–1063, http://dx.doi.org/10.1016/j.chemosphere.2013.05.078.
[41] D. Kaplan, D. Christiaen, S.M. Arad, Chelating properties of extracellular polysaccharides from *Chlorella* spp, Appl. Environ. Microbiol. 53 (12) (1987) 2953–2956.
[42] G. Gorbi, M. Invidia, C. Zanni, A. Torelli, M.G. Corradi, Bioavailability, bioaccumulation and tolerance of chromium: consequences in the food chain of freshwater ecosystems, Ann. Chim. 94 (2004) 505–513, http://dx.doi.org/10.1002/adic.200490064.
[43] V. Murphy, H. Hughes, P. Mcloughlin, Comparative study of chromium biosorption by red, green and brown seaweed biomass, Chemosphere 70 (2008) 1128–1134, http://dx.doi.org/10.1016/j.chemosphere.2007.08.015.
[44] F. Pagnanelli, M.P. Papini, L. Toro, M. Trifoni, F. Vegliò, Biosorption of metal ions on *Arthrobacter* sp.: biomass characterization and biosorption modeling, Environ. Sci. Technol. 34 (2000) 2773–2778, http://dx.doi.org/10.1021/es991271g.
[45] M.F. Sawalha, J.R. Peralta-Videa, G.B. Saupe, K.M. Dokken, J.L. Gardea-Torresdey, Using FTIR to corroborate the identity of functional groups involved in the binding of Cd and Cr to saltbush (*Atriplex canescens*) biomass, Chemosphere 66 (2007) 1424–1430, http://dx.doi.org/10.1016/j.chemosphere.2006.09.028.
[46] L.S. Ferreira, M.S. Rodrigues, J.C.M. de Carvalho, A. Lodi, E. Finocchio, P. Perego, A. Converti, Adsorption of Ni^{2+}, Zn^{2+} and Pb^{2+} Onto Dry Biomass of Arthrospira (Spirulina) Platensis and *Chlorella vulgaris*. I. Single Metal Systems, Elsevier B.V., 2011, http://dx.doi.org/10.1016/j.cej.2011.07.039.
[47] Y. Xu, Y. Fu, D. Zhang, Cost-effectiveness analysis on magnetic harvesting of algal cells, Mater. Today Proc. 4 (2017) 50–56, http://dx.doi.org/10.1016/j.matpr.2017.01.192.
[48] S. Ge, M. Agbakpe, W. Zhang, L. Kuang, Z. Wu, X. Wang, Recovering magnetic Fe_3O_4–ZnO nanocomposites from algal biomass based on hydrophobicity shift under UV irradiation, ACS Appl. Mater. Interfaces 7 (2015) 11677–11682, http://dx.doi.org/10.1021/acsami.5b03472.
[49] Y. Yang, J. Hou, P. Wang, C. Wang, L. Miao, Y. Ao, Y. Xu, X. Wang, B. Lv, G. You, Z. Yang, Interpretation of the disparity in harvesting efficiency of different types of *Microcystis aeruginosa* using polyethylenimine (PEI)-coated magnetic nanoparticles, Algal Res. 29 (2018) 257–265, http://dx.doi.org/10.1016/j.algal.2017.10.020.
[50] A. Chan, H. Salsali, E. McBean, Heavy metal removal (copper and zinc) in secondary effluent from wastewater treatment plants by microalgae, ACS Sustain. Chem. Eng. 2 (2014) 130–137, http://dx.doi.org/10.1021/sc400289z.
[51] J. Wang, S. Zheng, Y. Shao, J. Liu, Z. Xu, D. Zhu, Amino-functionalized Fe3O4@SiO2 core-shell magnetic nanomaterial as a novel adsorbent for aqueous heavy metals removal, J. Colloid Interface Sci. 349 (2010) 293–299, http://dx.doi.org/10.1016/j.jcis.2010.05.010.
[52] L. Weng, W.H. Van Riemsdijk, T. Hiemstra, Factors controlling phosphate interaction with iron oxides, J. Environ. Qual. 41 (2012) 628, http://dx.doi.org/10.2134/jeq2011.0250.
[53] P.P. Martin, M.F. Agosto, J.F. Bengoa, N.A. Fellenz, Zinc and chromium elimination from complex aqueous matrices using a unique aminopropyl-modified MCM-41 sorbent: temperature, kinetics and selectivity studies, J. Environ. Chem. Eng. 5 (2017) 1210–1218, http://dx.doi.org/10.1016/j.jece.2017.02.003.